Influence of waveguide geometry on scattering loss effects in submicron strip silicon-on-insulator waveguides

F. Grillot, L. Vivien, E. Cassan and S. Laval

Abstract: Silicon-on-insulator (SOI) optical waveguides with high electromagnetic field confinement suffer from side-wall roughness, which is responsible for strong scattering inducing propagation loss. A theoretical investigation of the influence of geometry in submicron SOI waveguides on the scattering loss due to side-wall roughness is reported. Scattering loss coefficient is derived for both narrow and flat SOI strip waveguides. It is shown that scattering loss coefficient is significantly increased for narrow waveguides compared with flatter ones. These results show that attention has to be paid to waveguide geometry, as scattering effects are the predominant source of optical losses in strip submicron SOI optical waveguides.

1 Introduction

Silicon-on-insulator (SOI) wafer is of prime importance for integrated optoelectronic circuits, as it offers potentiality for monolithic integration of optical and electronic functions on a single substrate. As silicon is transparent at wavelengths larger than 1.1 μm, including the optical communication bands, the silicon film of SOI substrates can be used to fabricate low-loss optical waveguides [1, 2]. Silicon/silicon dioxide (Si/SiO_2) waveguides benefit from a large refractive index difference, inducing high electromagnetic field confinement in the silicon-guiding layer which in turn allows to reduce the waveguide size to sub-micrometer values [3–6]. In order to use SOI waveguides for optical communications, both polarisation insensitivity and single-mode propagation have to be simultaneously fulfilled. It has been shown that these conditions can be reached when deeply etched rib SOI waveguides with dimensions of the order of 1 μm [7] are used. Because of the etching process realised by reactive ion etching (RIE), these devices generally suffer from side-wall roughness. Such a random phenomenon constitutes the dominant source of propagation loss [8]. In order to reduce side-wall roughness, the use of an oxidation step or of an anisotropic etching added to an RIE process has led to feasibility demonstration of SOI strip submicron waveguides with loss lower than 5 dB/cm [3]. Let us also note that by using a standard CMOS fabrication line, ultra-low propagation loss of 2.4 and 3.6 dB/cm have also been reported in strip SOI optical waveguides [4, 5]. In order to predict the influence of side-wall roughness on propagation loss, a model based on a planar optical waveguide was developed [8] and extended to the case of 2D Si/SiO_2 structures [9]. A numerical investigation of scattering loss induced by side-wall roughness as a function of the size of submicron SOI square strip waveguides has been performed [10]. It was shown that scattering loss strongly depends on the waveguide cross-section and decreases when the size is reduced below a given value because of a lower optical confinement. Thus, scattering loss is strongly correlated to the field confinement and the smallest structures can be useful for 3D tapers designed for low loss coupling between polarisation-insensitive microwaveguides and single-mode optical fibres [11, 12]. The aim of this paper is to propose a theoretical investigation serving to quantitatively estimate how scattering effects behave with the geometrical shape of submicron SOI waveguides. Thus, it is shown at the end of the paper that the scattering loss increase is more pronounced for deeply etched waveguides than for flatter ones. Although this result is quite expected, the proposed analysis is of first importance for the realisation and for the optimisation of nanodevices for optical telecommunications as well as for future optical interconnect in integrated circuits [13].

2 Description of the numerical model

The geometry of the strip optical waveguide under study is shown in Fig. 1. The silicon core layer (with optical index $n_c = 3.44$) is surrounded by a silica cladding (with optical index $n_{cl} = 1.44$). The waveguide cross-section is denoted as $2d_x \times 2d_y$ and the propagation wavenumber is $\beta = 2\pi n_{eff}/\lambda$ with n_{eff} the effective index and λ the operating wavelength fixed at 1.55 μm. It is important to emphasise that only the real part of the effective index is taken into account in the present work meaning leaky modes are not considered in the structure. Calculations are also performed for a transverse electrical polarisation of the incident fundamental mode. The influence of the polarization on the scattering loss coefficient will be discussed elsewhere.

Side-wall roughness is taken into account by assuming a random variation of the waveguide width. This leads to local variations of the effective index corresponding to the formation of a pseudo-grating along the side-wall. Thus, side-wall roughness acts as a dipole which can be excited by the incident waveguide mode. As a fraction of the

doi:10.1049/iet-opt:20070001

Paper first received 16th January and in revised form 23rd March 2007

F. Grillot is with Laboratoire d'Etudes des Nanostructures à Semiconducteurs, UMR CNRS FOTON, Institut National des Sciences Appliquées, 20 av. des Buttes de Coësmes, Rennes Cedex 35043, France

L. Vivien, E. Cassan and S. Laval are with Institut d'Electronique Fondamentale, UMR CNRS 8622, Université Paris-Sud, Orsay 91405, France

E-mail: frederic.grillot@insa-rennes.fr

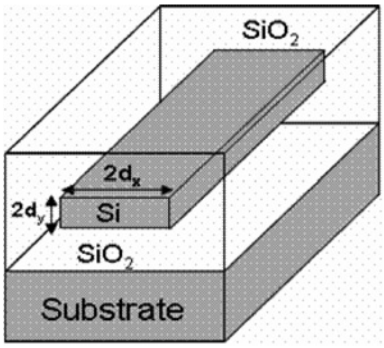

Fig. 1 *Strip waveguide geometry with $2d_x$ and $2d_y$ ranging from 150 to 1000 nm*

dipole cannot be recovered, scattering loss effects take place [14]. Scattering loss coefficient can be expressed following the well-known relation [8]

$$\alpha = \varphi^2(d)(n_c^2 - n_{cl}^2)^2 \frac{k_0^3}{4\pi n_c} \int_0^{\pi} \tilde{R}(\beta - n_{cl}k_0 \cos\theta)\,d\theta \quad (1)$$

where $\varphi^2(d)$ is a modal function depending only on the waveguide geometrical parameters and $k_0 = 2\pi/\lambda$ is the wavevector in vacuum. The integral term includes the power spectrum function $\tilde{R}(\Omega)$ ($\Omega = \beta - n_{cl}k_0\cos\theta$ with θ the scattering angle relative to the waveguide axis) which takes into account all the spatial frequencies Ω induced by side-wall roughness. Using the Wiener–Khintchine theorem for the calculation of the total radiated power, $\tilde{R}(\Omega)$ is linked to the autocorrelation function $R(u)$ through a Fourier transform [15]

$$\tilde{R}(\Omega) = \frac{1}{2\pi}\int_{-\infty}^{+\infty} R(u)\exp(i\Omega u)\,du \quad (2)$$

The autocorrelation function $R(u)$ takes into account the local variations of the effective index linked to the evolution of side-wall roughness and corresponds to a measurement of the average correlation between one position along the waveguide with another set at a distance u further along. The autocorrelation function is usually described either by an exponential or by a Gaussian statistic [14]. Experimental investigations have shown that an exponential statistic is well suited to characterise side-wall roughness of larger waveguides [16, 17], but to our knowledge, no experimental evidence has been yet reported for submicron ones. As a result, a side-wall roughness described by an exponential autocorrelation function is assumed in the following such as

$$R(u) = \sigma^2 \exp\left(-\frac{|u|}{L_c}\right) \quad (3)$$

with L_c the correlation length and σ the standard deviation. Using (3), analytical calculations can then be carried out and the scattering loss coefficient in dB/cm can be written as

$$\alpha_{dB/cm} = 4.34\frac{\sigma^2}{k_0\sqrt{2}d^4 n_c} g(V)f(x,\gamma) \quad (4)$$

where $g(V)$ is a function depending only on the waveguide geometry, whereas $f(x,\gamma)$ is linked to the side-wall roughness

$$g(V) = \frac{U^2V^2}{1+W} \quad (5)$$

with the normalised coefficients

$$U = k_0 d\sqrt{n_c^2 - n_{eff}^2} \quad (6a)$$

$$V = k_0 d\sqrt{n_c^2 - n_{cl}^2} \quad (6b)$$

$$W = k_0 d\sqrt{n_{eff}^2 - n_{cl}^2} \quad (6c)$$

and

$$f(x,\gamma) = \frac{x\sqrt{1 - x^2 + \sqrt{(1+x^2)^2 + 2x^2\gamma^2}}}{\sqrt{(1+x^2)^2 + 2x^2\gamma^2}} \quad (7)$$

where the normalised expressions of coefficients x, γ and Δ can be written as

$$x = W\frac{L_c}{d} \quad (8)$$

$$\gamma = \frac{n_{cl}V}{n_c W\sqrt{\Delta}} \quad (9)$$

$$\Delta = \frac{n_c^2 - n_{cl}^2}{2n_c^2} \quad (10)$$

Equation (4) shows that the propagation loss coefficient is linked to the roughness parameters σ and L_c. However, let us stress that this equation does not include the lateral field confinement. In order to take into account the 2D character of the SOI strip waveguides, the effective index n_{eff} is at first recalculated by using the film mode matching method which is well suited to high index contrast structures [18]. Then the scattering loss coefficient can be derived by injecting the effective index value directly into (4). It is also important to note that such a model does not take into account neither a 2D side-wall roughness nor scattering effects occurring both at the top and at the bottom of the waveguide. In the case of a more quantitative analysis, a 3D theoretical model based on the volume current method has recently been proposed to investigate scattering loss in microphotonic waveguides: it is shown that the change of the confinement both in the vertical and horizontal dimensions has to be taken into account to describe with more accuracy the vertical field profile along the rough side wall [19].

In what follows the 2D theoretical model is used and a numerical investigation is conducted: starting from a submicron square strip device, the waveguide cross-section is stretched through different configurations and scattering losses are calculated in all cases. A qualitative discussion illustrating the influence of the waveguide dimensions is conducted.

3 Numerical results and discussion

The starting point of this numerical study assumes a square SOI strip waveguide cross-section such as $2d_x = 2d_y = 2d = 150$ nm. Two different ways both leading to rectangular cross-sections are considered. The cross-section is stretched either vertically [case (i)] such as $150\text{ nm} \le 2d_y \le 1000$ nm (while the waveguide width remains constant to $2d_x = 150$ nm) or horizontally [case (ii)], namely $150\text{ nm} \le 2d_x \le 1000$ nm (while the etching height remains constant to $2d_y = 150$ nm). The influence of the etching height on scattering loss coefficient can be investigated from case (i). The second configuration where the etching height remains constant is used as a comparison.

However, it is important to note that whatever the situation, every variation of the waveguide geometry modifies the optical confinement, the effective index and then the scattering coefficient through (4). For instance, the predicted mode diameter is depicted in Fig. 2*a* for case (i) and in Fig. 2*b* for case (ii). As there is no evidence to get a circular optical mode with those structures, only the horizontal mode diameter is reported. In both situations, simulations show that the mode diameter calculated at $1/e^2$ is strongly linked to the waveguide dimensions. For instance, in Fig. 2*a*, the mode diameter decreases from 2.16 μm for a 150 nm × 150 nm square waveguide to 0.75 μm for a 150 nm × 1000 nm one. On the other hand, the calculated mode diameter reported in Fig. 2*b* is quite different: considering the same starting waveguide, the mode diameter decreases from 2.16 μm to a minimum equal to 0.4 μm for a 400 nm × 150 nm cross-section and then slightly increases to 0.85 μm for a 1000 nm × 150 nm one.

Calculated scattering loss coefficient is depicted against waveguide dimensions in Fig. 3. Both cases (i) (square marks) and (ii) (circle marks) are reported. Roughness parameters used in the calculations are $L_c = 50$ nm and $\sigma = 2$ nm. These parameters have been chosen according to measurements obtained on similar structures which have demonstrated a standard deviation close to 2 nm if an oxidation or anisotropic etching step is added to the RIE process [3]. At first, simulation shows that the square optical waveguide with a 150 nm × 150 nm cross-section exhibits ultra-low scattering loss which does not exceed 0.50 dB/cm. In this particular case, the effective index is so close to the refractive index of the silicon oxide cladding [20] that this behaviour can be attributed to a significant de-confinement of the optical mode which is favourable to loss reduction [10]. However, it is important to stress that such an advantage for a single SOI optical waveguide can be deleterious for coupled ones since a higher cross-talk will be obtained. A similar situation can also be expected with bend waveguides where the minimal bend radius for a certain bend loss will be seriously increased.

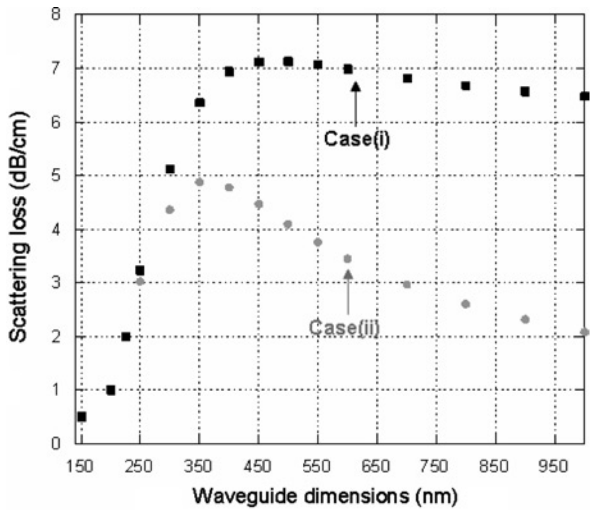

Fig. 3 *Calculated propagation loss against the waveguide width ($150\ nm < 2d_k < 500\ nm$, with $k = x$ or y) with roughness parameters $\sigma = 2$ nm and $L_c = 50$ nm for case (i) $150\ nm \leq 2d_y \leq 1000\ nm$; $2d_x = 150$ nm and for case (ii) $150\ nm \leq 2d_x \leq 1000\ nm$; $2d_y = 150$ nm*

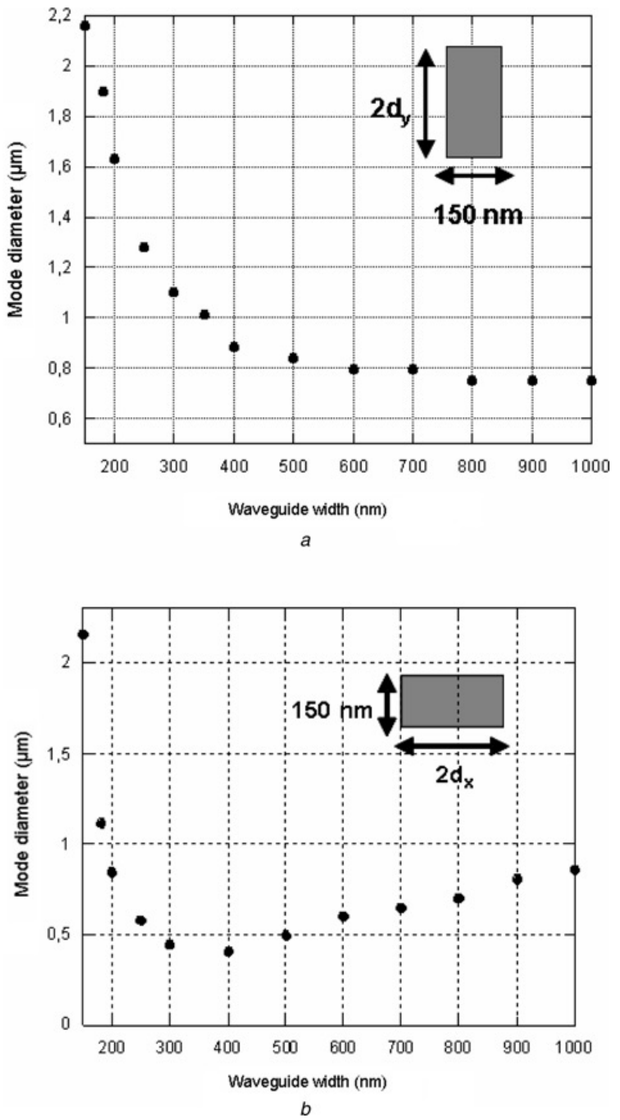

Fig. 2 *Calculated horizontal mode diameter as a function of waveguide dimensions for strip waveguides with the following cross-sections*

a 150 nm × $2d_y$, $150\ nm \leq 2d_y \leq 1000$ nm
b $2d_x$ × 150 nm, $150\ nm \leq 2d_x \leq 1000$ nm

Simulation also shows that in both cases scattering loss coefficient remains identical till the stretched dimensions reach 250 nm. Loss plots are superimposed and scattering loss monolithically increases due to the strengthened overlap of the optical field with waveguide side walls. This is consistent with the curves exhibited in Fig. 2 since the decrease in the mode diameter is much more pronounced for waveguide dimensions lower than 300 nm. The smaller the mode diameter, the stronger the interaction between the side walls and the optical mode and the higher the scattering loss coefficient. Nevertheless, when stretched dimensions go beyond 250 nm, losses tend to split. In both cases, scattering loss increases to reach a maximum whose position is induced by the waveguide geometry. Loss enhancement is more pronounced when the height of the side walls varies. For instance, scattering loss increases up to 6.5 dB/cm for a 150 nm × 1000 nm cross-section waveguide instead of 2 dB/cm for a 1000 nm × 150 nm one. This result is expected and attributed to the interaction of the optical mode with the waveguide side walls which is much more important for narrow waveguides than for larger ones. For case (i), simulations presented in Fig. 2*a* show that when the waveguide height goes beyond 400 nm, the optical confinement tends to a constant with a mode diameter equal to 0.85 μm. As a result, the scattering loss coefficient (Fig. 3) is roughly constant above 400 nm. On the other hand, simulations in Fig. 2*b* show that the behaviour of the optical confinement is quite different than that for case (ii). Because of the horizontally stretching, the mode diameter decreases to a minimum around 350 nm and starts increasing after. This can be correlated with Fig. 3 where the scattering loss coefficient starts decreasing after 350 nm because of a lower optical confinement.

Further investigations have been made to estimate the overall scattering loss coefficient for large variation of the roughness parameters σ and L_c. Assuming $0 \leq L_c \leq 100$ nm and $0 \leq \sigma \leq 10$ nm, contour lines of scattering loss are reported in the (σ, L_c) plane for a 150 nm × 500 nm (Fig. 4*a*) and 500 nm × 150 nm (Fig. 4*b*). Such waveguide dimensions have been chosen because they correspond to typical sizes of submicron strip SOI devices [6, 7]. At first, simulations show that depending on the position chosen in the diagram either the influence of L_c or that of σ is stronger meaning that both L_c and σ have to be taken into account to correctly describe side-wall roughness. It can also be seen that scattering loss calculated in Fig. 4*a* is higher than that calculated in Fig. 4*b*. For example, for $L_c = 50$ nm and $\sigma = 6$ nm, calculated scattering loss goes beyond 60 dB/ cm in Fig. 4*a*, whereas it does not exceed 40 dB/cm in Fig. 4*b*. This difference of hardly two orders of magnitude is again induced by the interaction of the optical mode with the side walls which is much more important for a 150 nm × 500 nm narrow waveguide than for a 500 nm × 150 nm larger one. These simulation results point out the importance of an accurately controlled fabrication process since a variation of the standard deviation induced by a larger fluctuation amplitude at the core/cladding interfaces leads to stronger scattering effects. This numerical investigation also shows that whatever the amplitude of side-wall roughness, scattering loss coefficient is drastically enhanced for narrow and high waveguides.

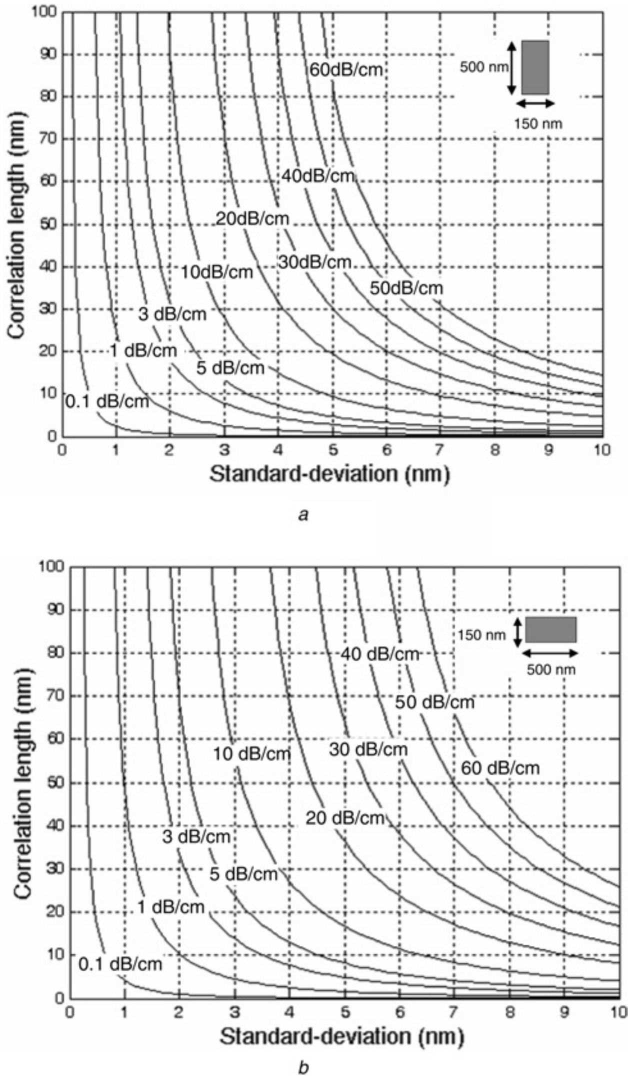

Fig. 4 *Contour lines of the propagation loss in the (σ, L_c) plane for two strip waveguide cross-sections*

a $2d_x \times 2d_y = 150$ nm × 500 nm
b $2d_x \times 2d_y = 500$ nm × 150 nm

4 Conclusions

In conclusion, this numerical investigation shows that attention has to be paid to the influence of the waveguide geometry on the scattering effects which are the predominant source of optical losses in strip submicron SOI optical waveguides. By taking into account the roughness parameters and starting from an ultra-low loss submicron square waveguide, it has been shown that scattering loss coefficient increases when the waveguide is stretched in one direction. Part of this enhancement has been attributed to the optical confinement which changes with the waveguide geometry. Another part is due to the rough side-wall area which is more pronounced for deeply etched waveguides than for flatter ones. As a conclusion, this qualitative analysis illustrating the influence of the waveguide dimensions opens the way for designing and optimising a wide range of nanowaveguide geometries. These nanodevices used both for optical communications and for future optical interconnects definitely require a quantitative evaluation of the scattering loss coefficient before processing.

5 References

1 Layadi, A., Vonsovici, A., Orobtchouk, R., Pascal, D., and Koster, A.: ‘Low-loss optical waveguide on standard SOI/SIMOX substrate’, *Opt. Commun.*, 1998, **146**, pp. 31–33
2 Schmidtchen, J., Splett, A., Schuppert, B., Petermann, K., and Burbach, G.: ‘Low loss singlemode optical waveguides with large cross-section in silicon-on-insulator’, *Electron. Lett.*, 1991, **27**, pp. 1486–1488
3 Lee, K.K., Lim, D.R., Kimerling, L.C., Shin, J., and Cerrina, F.: ‘Fabrication of ultralow-loss Si/SiO_2 waveguides by roughness reduction’, *Opt. Lett.*, 2001, **26**, pp. 1888–1890
4 Dumon, P., Bogaerts, W., Wiaux, V., Wouters, J., Beckx, S., Van Campenhout, J., Taillaert, D., Luyssaert, B., Bienstman, P., Van Thourhout, D., and Baets, R.: ‘Low-loss SOI photonic wires and ring resonators fabricated with deep UV lithography’, *IEEE Photonics. Technol. Lett.*, 2004, **16**, pp. 1328–1330
5 Vlasov, Y.A., and McNab, S.J.: ‘Losses in single-mode silicon-on-insulator strip waveguides and bends’, *Opt. Express.*, 2004, **12**, pp. 1622–1631
6 Lardenois, S., Pascal, D., Vivien, L., Cassan, E., Laval, S., Orobtchouk, R., Heitzmann, M., Bouzaida, N., and Mollard, L.: ‘Low-loss submicrometer silicon-on-insulator rib waveguides and corner mirrors’, *Opt. Lett.*, 2003, **28**, pp. 1150–1152
7 Vivien, L., Laval, S., Dumont, B., Lardenois, S., Koster, A., and Cassan, E.: ‘Polarization-independent single-mode rib waveguides on silicon-on-insulator for telecommunication wavelengths’, *Opt. Commun.*, 2002, **210**, pp. 43–49
8 Payne, F.P., and Lacey, J.P.R.: ‘Radiation loss from planar waveguides with random wall imperfections’, *IEE Proc., Optoelectron.*, 1990, **137**, pp. 282–288
9 Lee, K.K., Lim, D.R., Luan, H.C., Agrawal, A., Foresi, J., and Kimerling, L.C.: ‘Effect of size and roughness on light transmission in a Si/SiO_2 waveguide: experiments and model’, *Appl. Phys. Lett.*, 2000, **77**, pp. 1617–1619
10 Grillot, F., Vivien, L., Laval, S., Pascal, D., and Cassan, E.: ‘Size influence on the propagation loss induced by side-wall roughness in ultra-small SOI waveguides’, *IEEE Photonics Technol. Lett.*, 2004, **16**, pp. 1661–1663
11 Vivien, L., Laval, S., Cassan, E., Le Roux, X., and Pascal, D.: ‘2-D taper for low-loss coupling between polarization-insensitive microwaveguides and single-mode optical fibers’, *J. Light Technol.*, 2003, **21**, pp. 2429–2433

12 Vivien, L., Le Roux, X., Laval, S., Cassan, E., and Marris-Morini, D.: 'Design, Realization, and characterization of 3D taper for fiber/micro-waveguide coupling', *J. Sel. Top. Quantum Electron.*, 2006, **12**, (6), pp. 1354–1358

13 Marris, D., Vivien, L., Pascal, D., Rouvière, M., Cassan, E., Lupu, A., Laval, S., Fédéli, J.M., and El Melhaoui, L.: 'Ultralow loss successive divisions using silicon-on-insulator microwaveguides', *Appl. Phys. Lett.*, 2005, **87**, p. 211102

14 Boagaerts, W., Bienstman, P., and Baets, R.: 'Scattering at sidewall roughness in photonic crystal slabs', *Opt. Lett.*, 2003, **28**, pp. 689–691

15 Ladouceur, F., Love, J.D., and Senden, T.J.: 'Effect of side wall roughness in buried channel waveguides', *IEE Proc., Optoelectron.*, 1994, **141**, pp. 242–248

16 Ladouceur, F., Love, J.D., and Senden, T.J.: 'Measurement of surface roughness in buried channel waveguides', *Electron. Lett.*, 1992, **28**, pp. 1321–1322

17 Ladouceur, F.: 'Roughness, inhomogeneity, and integrated optics', *J. Light Technol.*, 1997, **15**, pp. 1020–1025

18 'FIMMWAVE software: Photon Design', available at: www.photond.com, 2006

19 Barwicz, T., and Haus, H.A.: 'Three dimensional analysis of scattering losses due to sidewall roughness in microphotonic wavaguides', *J. Light Technol.*, 2005, **23**, pp. 2719–2732

20 Grillot, F., Vivien, L., Laval, S., and Cassan, E.: 'Propagation loss in single-mode ultra-small square silicon-on-insulator optical waveguides', *J. Light Technol.*, 2006, **24**, pp. 891–896